Magnetocaloric effect under applied pressure and the barocaloric effect in the compounds RCo_2 (R = Er, Ho and Dy)

2008 J. Phys.: Condens. Matter 20 175209

(http://iopscience.iop.org/0953-8984/20/17/175209)

J. Phys.: Condens. Matter **20** (2008) 175209 (6pp) doi:10.1088/0953-8984/20/17/175209

Magnetocaloric effect under applied pressure and the barocaloric effect in the compounds RCo_2 (R = Er, Ho and Dy)

N A de Oliveira

Universidade do Estado do Rio de Janeiro, Instituto de Física Armando Dias Tavares, Rua São Francisco Xavier 524, Rio de Janeiro, 20550-013, RJ, Brazil

Received 25 October 2007, in final form 29 February 2008
Published 3 April 2008
Online at stacks.iop.org/JPhysCM/20/175209

Abstract

In this work, I discuss the magnetocaloric effect under applied pressure, as well as the barocaloric effect, in the Laves phase compounds RCo_2 (R = Er, Ho and Dy). To this end, I use a model Hamiltonian including both localized 4f spins and itinerant 3d electrons. The calculations point out that (i) for an applied pressure of 1.0 GPa the peaks of the magnetocaloric potentials $[\Delta S]_M$ and $[\Delta T_{ad}]_M$ are shifted to lower temperatures, but their magnitudes remain almost unchanged; (ii) the magnetocaloric potentials exhibit sizable values in a wider range of temperatures, when both magnetic field and pressure are changed; (iii) the peaks of the barocaloric potentials $[\Delta S]_B$ and $[\Delta T_{ad}]_B$ can be as large as the magnetocaloric ones.

1. Introduction

The magnetocaloric effect [1, 2] is intrinsic to all magnetic materials and is basically the entropy change due to the application of an external magnetic field. The magnetocaloric effect is characterized by the isothermal entropy change $[\Delta S]_M$ and by the adiabatic temperature change $[\Delta T_{ad}]_M$ upon magnetic field variation. The barocaloric effect [3, 4] is the entropy change due to the application of an external pressure. The barocaloric effect is characterized by the isothermal entropy change $[\Delta S]_B$ and by the adiabatic temperature change $[\Delta T_{ad}]_B$ upon pressure variation. The magnetocaloric effect in the Laves phase intermetallic compounds RCo_2 has already been studied in the literature [5–12]. Experimental and theoretical works show that at ambient pressure the compounds $ErCo_2$, $HoCo_2$ and $DyCo_2$, which undergo a first order magnetic phase transition, exhibit large values of the isothermal entropy change around the magnetic ordering temperature. However, the magnetocaloric effect under applied pressure and the barocaloric effect in these compounds have not been studied yet.

In this work, the barocaloric effect and the magnetocaloric effect under applied pressure in the compounds RCo_2, (R = Er, Ho and Dy) are theoretically discussed. To this end, a model Hamiltonian taking into account both the localized 4f spins of rare earth ions and itinerant 3d electrons of the Co ions is used. The crystalline electrical field effect on the 4f ground multiplet of the rare earth ions was also included in the model. The effect of the magnetoelastic interaction on the rare earth ions was considered in the framework of the Kittel model [13]. On the other hand, the effect of the magnetoelastic interaction on the itinerant electrons was considered in the framework of the model developed by Duc *et al* [14]. The effect of an applied pressure was phenomenologically included via the exchange interaction integral between 4f spins and via the dispersion relation of itinerant electrons.

The theoretical calculations of the magnetocaloric potentials $[\Delta S]_M$ and $[\Delta T_{ad}]_M$ at ambient pressure in the compounds $ErCo_2$, $HoCo_2$ and $DyCo_2$ are in good agreement with the available experimental data [6, 15]. Besides, the theoretically calculated magnetocaloric potentials $[\Delta S]_M$ and $[\Delta T_{ad}]_M$ under simultaneous variation of the magnetic field and pressure exhibit large values in a wider range of temperatures. The calculations also show that the barocaloric potentials $[\Delta S]_B$ and $[\Delta T_{ad}]_B$ in these compounds can be as large as the magnetocaloric potentials $[\Delta S]_M$ and $[\Delta T_{ad}]_M$ at ambient pressure. These findings open a brand new horizon in the study of the magnetocaloric effect and the barocaloric effect in compounds undergoing a first order phase transition.

2. Formulation

The starting point to calculate the magnetocaloric effect in the series of compounds RCo_2 is the model Hamiltonian

$\mathcal{H} = \mathcal{H}_{\rm d} + \mathcal{H}_{\rm f}$, where

$$\mathcal{H}_{\rm d} = \sum_{i\sigma} \varepsilon_{0\sigma} d^{+}_{i\sigma} d_{i\sigma} + \sum_{il\sigma} T_{il\sigma} d^{+}_{i\sigma} d_{l\sigma} + U \sum_{i} n^{\rm d}_{i\uparrow} n^{\rm d}_{i\downarrow} + \tfrac{1}{2} \sum_{i} \lambda_{\rm df} \vec{J}^{\rm f}_{i} \cdot \vec{s}^{\rm d}_{i} - \sum_{i} g^{\rm d} \mu_{\rm B} \vec{B} \cdot \vec{s}^{\rm d}_{i} \quad (1)$$

and

$$\mathcal{H}_{\rm f} = -\sum_{il} \lambda_{il}(r) \vec{J}^{\rm f}_{i} \cdot \vec{J}^{\rm f}_{l} - \sum_{i} g^{\rm f} \mu_{\rm B} \vec{B} \cdot \vec{J}^{\rm f}_{i} + \tfrac{1}{2} \sum_{i} \lambda_{\rm df} \vec{J}^{\rm f}_{i} \cdot \vec{s}^{\rm d}_{i} + \sum_{i} \mathcal{H}^{\rm CF}_{i}. \quad (2)$$

The Hamiltonian $\mathcal{H}_{\rm d}$ describes the itinerant electrons, where the first term is a reference energy; the second term describes the electron hopping, where $T_{il\sigma} = \sum_{k} \tilde{\varepsilon}_{k\sigma} {\rm e}^{{\rm i}k(R_i - R_l)}$ is the electron hopping energy, and $\tilde{\varepsilon}_{k\sigma}$ is a renormalized electron dispersion relation. The third term describes the electron–electron interaction, where U is the Coulomb interaction parameter. The fourth term describes the coupling with the 4f spins, where $\lambda_{\rm df}$ is an exchange interaction parameter. The last term describes the coupling with the applied magnetic field (B), where $\mu_{\rm B}$ is the Bohr magneton and $g^{\rm d}$ is the Landé factor of the itinerant electrons. The Hamiltonian $\mathcal{H}_{\rm f}$ describes a subsystem of localized 4f spins, where the first term describes the interaction between rare earth ions, where $J^{\rm f}_{i}$ is the total angular momentum of rare earth ions and λ_{il} is the exchange interaction integral. The second term represents the Zeeman interaction between the rare earth total angular momentum and the applied magnetic field, where $g^{\rm f}$ is the Land é factor of rare earth ions. The third term describes the coupling between rare earth spin and the spin of the itinerant electrons. The last term describes the crystalline electrical field effect on the 4f ground multiplet of the rare earth ions. For the cubic symmetry, the crystalline electrical field Hamiltonian $\mathcal{H}^{\rm CF}$ is given by [16] $\mathcal{H}^{\rm CF}_{i} = W[x(O^0_4 + 5O^4_4)/F_4 + (1 - |x|)(O^0_6 - 21O^4_6)/F_6]_i$, where W is an energy scale and x gives the relative importance of the fourth and sixth order terms. O^n_m are the Stevens operators [17]; F_4 and F_6 are numerical factors common to all matrix elements.

The exchange interaction integral λ_{il} depends on the distance between neighboring sites in the crystalline lattice. As the temperature is increased, lattice vibrations take place, changing the distance between neighboring sites and consequently the exchange interaction integral. The exchange interaction integral can be written as [13] $\lambda(r) = \lambda_0(r_0) + \lambda_1(r_0) J^{\rm f}_{i} \cdot J^{\rm f}_{l}$, where λ_0 is the bare value of the exchange interaction integral, which depends on the fixed position (r_0) of the ions in the crystalline lattice. $\lambda_1(r_0) = \kappa[({\rm d}\lambda(r)/{\rm d}r)^2]_{r=r_0}$, where κ is a proportionality constant, depends on the vibrations of the ions. Applied pressure also changes the distance between neighboring sites so that the exchange interaction integral and consequently the magnetic ordering temperature will be a function of pressure. The effect of applied pressure is phenomenologically incorporated in the model through the renormalization of the parameters λ_0 and λ_1 in the form $\tilde{\lambda}_0 = \alpha_0\lambda_0$ and $\tilde{\lambda}_1 = \alpha_1\lambda_1$, where α_0 and α_1 are proportionality constants. Using $\lambda = \tilde{\lambda}_0 + \tilde{\lambda}_1 J^{\rm f}_{i} \cdot J^{\rm f}_{l}$ and taking the mean field approximation for the spin–spin interaction, the Hamiltonian $\mathcal{H}_{\rm f}$ can be explicitly written as

$$\begin{aligned}\mathcal{H}^{\rm MF}_{\rm f} = &-\sum_{i} \big[\lambda^{\rm eff}_0 \langle J^{\rm f}_x\rangle + \lambda^{\rm eff}_1 \langle J^{\rm f}_x\rangle^3 \\ &- 0.5\lambda_{\rm df}\langle s^{\rm d}\rangle + g^{\rm f}\mu_{\rm B}B\cos\delta\big] J^{\rm f}_{ix} \\ &- \sum_{i} \big[\lambda^{\rm eff}_0 \langle J^{\rm f}_y\rangle + \lambda^{\rm eff}_1 \langle J^{\rm f}_y\rangle^3 \\ &- 0.5\lambda_{\rm df}\langle s^{\rm d}\rangle + g^{\rm f}\mu_{\rm B}B\cos\theta\big] J^{\rm f}_{iy} \\ &- \sum_{i} \big[\lambda^{\rm eff}_0 \langle J^{\rm f}_z\rangle + \lambda^{\rm eff}_1 \langle J^{\rm f}_z\rangle^3 \\ &- 0.5\lambda_{\rm df}\langle s^{\rm d}\rangle + g^{\rm f}\mu_{\rm B}B\cos\varphi\big] J^{\rm f}_{iz} + \sum_{i} \mathcal{H}^{\rm CF}_{i}. \end{aligned} \quad (3)$$

This mean field Hamiltonian describes a sublattice of rare earth ions under the action of the external magnetic field and the effective fields $\langle J^{\rm f}\rangle$ and $\langle s^{\rm d}\rangle$. Here $\lambda^{\rm eff}_0 = \alpha_0\lambda_0 Z_n$ and $\lambda^{\rm eff}_1 = \alpha_1\lambda_1 Z_n$, where Z_n is the number of nearest neighbors. δ, θ and φ are the angles between the applied magnetic field direction and the crystallographic axes x, y and z respectively. For the sake of simplicity, the anisotropy in the mean value $\langle s^{\rm d}\rangle$ and in the exchange parameters λ_0 and λ_1 is neglected. The mean value $\langle J^{\rm f}_k\rangle$ ($k = x, y, z$) in equation (3) is calculated by $\langle J^{\rm f}_k\rangle = (\sum_j \langle E_j \mid J^{\rm f}_k \mid E_j\rangle {\rm e}^{-\beta E_j})/\sum_j {\rm e}^{-\beta E_j}$, where $\beta = 1/k_{\rm B}T$ with $k_{\rm B}$ being the Boltzmann constant. E and $|E\rangle$ are respectively the energy eigenvalues and eigenvectors of the mean field Hamiltonian $\mathcal{H}^{\rm MF}_{\rm f}$. In order to calculate the mean value $\langle s^{\rm d}\rangle$ associated with the Co sublattice it is necessary to know the 3d-electron dispersion relation, which is also affected by the lattice vibrations through the electron–phonon interaction. For the sake of simplicity, it is considered that the lattice vibrations renormalize the electron dispersion relation through a temperature dependent parameter [18] $[1-\gamma^{\rm el}(M^{\rm 3d})^2]$, where $M^{\rm 3d}$ is the magnetization of the Co sublattice and $\gamma^{\rm el}$ is a magnetoelastic coupling parameter. The effect of an applied pressure on the electron dispersion relation is incorporated in the model through the parameter $\alpha_{\rm el}$. Therefore, the renormalized electron dispersion relation, taking into account the effect of an external pressure and lattice vibrations, is given by $\tilde{\varepsilon}_k = \alpha_{\rm el}[1 - \gamma^{\rm el}(M^{\rm 3d})^2]\varepsilon_k$. Taking the mean field approximation and using $s_i = (1/2)\sum_\sigma \sigma n_{i\sigma}$ and $g^{\rm d} = 2$, the Hamiltonian $\mathcal{H}_{\rm d}$ turns out to be

$$\mathcal{H}^{\rm MF}_{\rm d} = \sum_{i\sigma} (\varepsilon_0 + U\langle n^{\rm d}_{-\sigma}\rangle + 0.25\sigma\lambda_{\rm df}\langle J^{\rm f}\rangle - \sigma\mu_{\rm B}B) d^{+}_{i\sigma} d_{i\sigma} + \sum_{il\sigma} T_{il\sigma} d^{+}_{i\sigma} d_{l\sigma}. \quad (4)$$

The local Green's function for the above Hamiltonian is given by [18]

$$g^{\rm 3d}_{00\sigma}(z) = \int \{\rho_0(\varepsilon')\,{\rm d}\varepsilon'\}\{z - \alpha_{\rm el}[1 - \gamma^{\rm el}(M^{\rm 3d})^2]\varepsilon' - \varepsilon_0 - U\langle n^{\rm d}_{-\sigma}\rangle - 0.25\sigma\lambda_{\rm df}\langle J^{\rm f}\rangle + \sigma\mu_{\rm B}B\}^{-1} \quad (5)$$

where $z = \varepsilon + {\rm i}0$ and $\rho_0(\varepsilon')$ is a standard paramagnetic density of states. The spin dependent density of states for 3d electrons is calculated by $\rho^{\rm 3d}_\sigma(\varepsilon) = -\frac{1}{\pi}\,{\rm Im}\, g^{\rm 3d}_{00\sigma}(z)$. The magnetization at the Co sublattice is calculated by $M^{\rm 3d}(T, B, p) = 5(\langle n^{\rm 3d}_\uparrow\rangle - \langle n^{\rm 3d}_\downarrow\rangle)$, where the factor of five accounts for the degeneracy of the 3d states. The electron occupation number per spin

direction is given by $\langle n_\sigma^{3d}\rangle = \int \rho_\sigma^{3d}(\varepsilon) f(\varepsilon)\, d\varepsilon$, where $f(\varepsilon)$ is the Fermi distribution function.

The magnetization at the rare earth sublattice is calculated by $M^{4f}(T, B, p) = g^f \mu_B \langle J^f\rangle$, where $\langle J^f\rangle = [\langle J_x^f\rangle^2 + \langle J_y^f\rangle^2 + \langle J_z^f\rangle^2]^{1/2}$. The magnetization at the Co sublattice (M^{3d}) and the magnetization at the rare earth sublattice (M^{4f}) should be self-consistently determined. For initial values of $\langle J_x^f\rangle$, $\langle J_y^f\rangle$, $\langle J_z^f\rangle$ and $\langle s^d\rangle$, the energies eigenvalues and eigenvectors (E; $|E\rangle$) are calculated from the mean field Hamiltonian $\mathcal{H}_f^{MF}$ and then used to obtain new values for $\langle J^f\rangle$. After this, the magnetization at the Co sublattice is calculated and the mean value $\langle s^d\rangle$ is obtained through the relation $\langle s^d\rangle = M^{3d}/g^d\mu_B$. This self-consistent process is repeated until two consecutive mean values of $\langle J^f\rangle$ and $\langle s^d\rangle$ are obtained within a numerical precision of 0.001.

After solving the self-consistency, the total magnetization of the compound RCo_2 is calculated from $M(T, B, p) = M^{4f}(T, B, p) + 2M^{3d}(T, B, p)$. The total entropy is given by $S(T, B, p) = S_{mag}^{4f}(T, B, p) + S_{mag}^{3d}(T, B, p) + S_{lat}(T, B, p)$, where $S_{mag}^{4f}(T, B, p)$ is the contribution from the rare earth ions [11], $S_{mag}^{3d}(T, B, p)$ represents the contribution from the Co ions [18] and $S_{lat}(T, B, p)$ represents the contribution from the crystalline lattice [18]. Once the total entropy is known, the magnetocaloric potentials $[\Delta S]_M$ and $[\Delta T_{ad}]_M$ for a fixed pressure and upon magnetic field variation $\Delta B = B_2 - B_1$ are calculated by $[\Delta S]_M = S(T, B_2, p) - S(T, B_1, p)$ and $[\Delta T_{ad}]_M = T_2 - T_1$ under the adiabatic condition $S(T_2, B_2, p) = S(T_1, B_1, p)$. In the case where both magnetic field and pressure are changed, the magnetocaloric potentials $[\Delta S]_M$ and $[\Delta T_{ad}]_M$ are respectively calculated by $[\Delta S]_M = S(T, B_2, p_2) - S(T, B_1, p_1)$ and $[\Delta T_{ad}]_M = T_2 - T_1$ under the adiabatic condition $S(T_2, B_2, p_2) = S(T_1, B_1, p_1)$. The barocaloric potentials [3, 4] $[\Delta S]_B$ and $[\Delta T_{ad}]_B$ for a fixed magnetic field and upon pressure variation $\Delta p = p_2 - p_1$ are calculated by $[\Delta S]_B = S(T, B, p_2) - S(T, B, p_1)$ and $[\Delta T_{ad}]_B = T_2 - T_1$ under the adiabatic condition $S(T_2, B, p_2) = S(T_1, B, p_1)$.

3. Results and discussion

In order to calculate the magnetocaloric effect in the Laves phase compounds $ErCo_2$, $HoCo_2$ and $DyCo_2$ it is necessary to fix a set of model parameters. The total angular momentum and the Landé factor were taken from the Hund rule. The number of first nearest neighbors Z_n, the coupling parameter λ_{df} and the factors [16] F_4 and F_6 were respectively taken as $Z_n = 10$, $\lambda_{df} = 0.2$ meV, $F_4 = 60$ and $F_6 = 13\,860$ for all three compounds. The exchange interaction parameters (λ_0 and λ_1) and the crystalline electric field parameters (x and W) used in the calculations are shown in table 1.

For describing the 3d electrons at the Co sites, a standard paramagnetic density of states [19] was adopted. The Coulomb interaction parameter was taken as $U = 0.2$, in units of the 3d bandwidth, and the number of electrons at the Co site was taken as $n = 1.6$. The input parameters for the Co sublattice were taken to assure that the Stoner criterion of the itinerant magnetism (i.e., $U\rho^{3d}(\varepsilon_F) > 1$) is not fulfilled. The magnetic field was applied along the $\langle 111\rangle$ direction for the compounds $ErCo_2$ and $DyCo_2$ and along the $\langle 100\rangle$ direction for $HoCo_2$. The bare value of the Debye temperature was taken as $\Theta = 230$ K for the compounds $ErCo_2$ and $HoCo_2$ and $\Theta = 200$ K for the compound $DyCo_2$. The magnetoelastic coupling parameter was taken as $\gamma^{el} = 0.1$ for all three compounds. The effect of an applied pressure of 1.0 GPa in $ErCo_2$, $HoCo_2$ and $DyCo_2$ was described by the set of parameters [$\alpha_0 = 0.709$; $\alpha_1 = 0.769$]; [$\alpha_0 = 0.696$; $\alpha_1 = 0.600$] and [$\alpha_0 = 0.912$; $\alpha_1 = 0.880$] respectively. For ambient pressure $\alpha_0 = \alpha_1 = 1.0$ for all compounds.

Table 1. Exchange interaction parameters (λ_0 and λ_1) and the crystalline electric field parameters (x and W) for the compounds $ErCo_2$, $HoCo_2$ and $DyCo_2$.

Compound	λ_0 (meV)	λ_1 (meV)	x	W (meV)
$ErCo_2$	0.0155	0.0013	−0.24	−0.042 14
$HoCo_2$	0.0330	0.0025	−0.4687	0.051 702
$DyCo_2$	0.0580	0.0017	−0.24	−0.042 14

The theoretical calculations for the chosen set of model parameters show that at ambient pressure the compounds $ErCo_2$, $HoCo_2$ and $DyCo_2$ undergo a first order magnetic phase transition around 33 K, 80 K and 135 K respectively. In figures 1(a) and (b) are respectively plotted the magnetocaloric potentials $[\Delta S]_M$ and $[\Delta T_{ad}]_M$ calculated upon magnetic field variation from 0 to 5 T at ambient pressure (solid lines) and for an applied pressure of 1.0 GPa (dashed lines). Notice that the agreement between the theoretical calculations and the available experimental data [6, 15] (symbols) at ambient pressure is very good. However, the change of sign experimentally observed at low temperature in the magnetocaloric curves of $HoCo_2$ is not reproduced by the present calculations. In order to theoretically obtain the anomaly at low temperature, which is due to the change of the easy magnetization direction [20] from $\langle 110\rangle$ at low temperatures to $\langle 100\rangle$ at temperatures above 14 K, it is necessary to self-consistently calculate the magnetoelastic coupling parameter in terms of the electronic structure of the compound. However, this kind of calculation is more complex and is not in the scope of the present work.

I have also calculated the magnetocaloric potentials $[\Delta S]_M$ and $[\Delta T_{ad}]_M$ in $ErCo_2$ when both magnetic field and pressure are changed. I have chosen four particular procedures to change the magnetic field and applied pressure. In the first process, the compound is initially under constant magnetic field ($B = 0$ or 5 T) at high temperature and ambient pressure. When the temperature goes down, an applied pressure of 1.0 GPa is suddenly applied at 25.5 K and kept fixed until 0 K. In this particular case of magnetic field and pressure variation, the magnetocaloric potentials $[\Delta S]_M$ and $[\Delta T_{ad}]_M$ exhibit two peaks (dashed lines in figures 2(a) and (b) respectively). The unusual second peak at low temperature occurs because when the pressure of 1.0 GPa is suddenly applied at 25.5 K the magnetic order is destroyed so that the magnetocaloric potentials go to zero. As the temperature decreases somewhat more, the magnetic order is again established so that the magnetocaloric potentials get large values, giving rise to

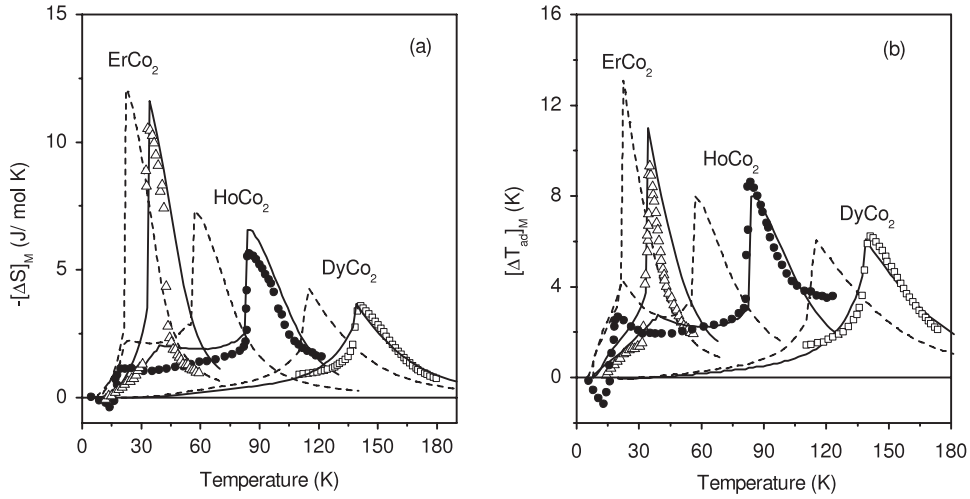

Figure 1. Magnetocaloric potentials $[\Delta S]_{\mathrm{M}}$ (a) and $[\Delta T_{\mathrm{ad}}]_{\mathrm{M}}$ (b) in the compounds $ErCo_2$, $HoCo_2$ and $DyCo_2$ for magnetic field variation from 0 to 5 T. Solid and dashed lines are the theoretical calculations for $p = 0$ and $p = 1.0$ GPa respectively. Symbols represent the available experimental data [6, 15].

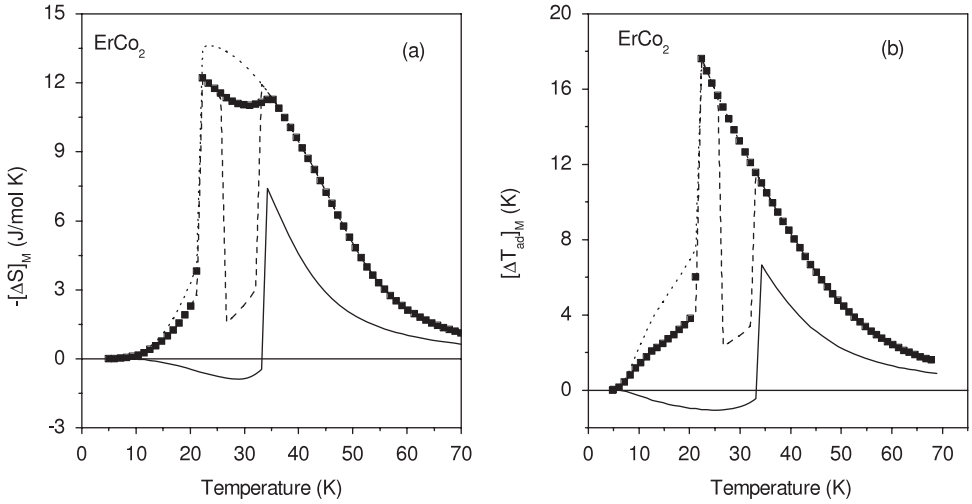

Figure 2. Magnetocaloric potentials $[\Delta S]_{\mathrm{M}}$ (a) and $[\Delta T_{\mathrm{ad}}]_{\mathrm{M}}$ (b) in the compound $ErCo_2$ for magnetic field and pressure variation. Dashed lines, squares, dotted lines and solid lines represent respectively the calculations for the first, second, third and fourth processes of magnetic field and pressure variation (see text for details).

the second peak in the magnetocaloric curves. It should be emphasized that the second peak appears because the chosen temperature of 25.5 K to change the applied pressure lies around the magnetic ordering temperature. However, if the pressure is applied at a given temperature far from this magnetic ordering temperature, the two peaks in the magnetocaloric curves disappear.

In the second process, the compound is initially under constant magnetic field ($B = 0$ or 5 T) at high temperature and ambient pressure. When the temperature goes down, an external pressure is smoothly applied from 0 to 1.0 GPa in the temperature interval from 35 to 25.5 K. Below 25.5 K the pressure is kept constant at 1.0 GPa. This process is shown by curve 1 of figure 3. With this particular choice of the magnetic field and pressure variation, the magnetocaloric potential $[\Delta S]_{\mathrm{M}}$ exhibits an almost constant value in a wider temperature range, as is represented by the squares in figure 2(a). This type of behavior in the $[\Delta S]_{\mathrm{M}}$ curves occurs due to the competition between the decrease of temperature and the smooth increase of the applied pressure in the establishment of the magnetic order.

In the third process, a pressure of 1.0 GPa is applied in the absence of an external magnetic field ($B = 0$) for the whole range of temperatures, while for a magnetic field of 5 T there is no pressure applied. In this case, the magnetocaloric potentials $[\Delta S]_{\mathrm{M}}$ and $[\Delta T_{\mathrm{ad}}]_{\mathrm{M}}$ also exhibit large values in a wider range of temperatures (dotted lines in figures 2(a) and (b)). In the fourth process, a pressure of 1.0 GPa is applied when the magnetic field is 5 T, while no pressure is applied when the magnetic field is absent. In this case, there is a change of sign in the $[\Delta S]_{\mathrm{M}}$ and $[\Delta T_{\mathrm{ad}}]_{\mathrm{M}}$ curves at a given temperature (solid lines in figures 2(a) and (b)). This anomaly is due to the competition between the magnetic field and pressure in the establishment of the magnetic order. It disappears as

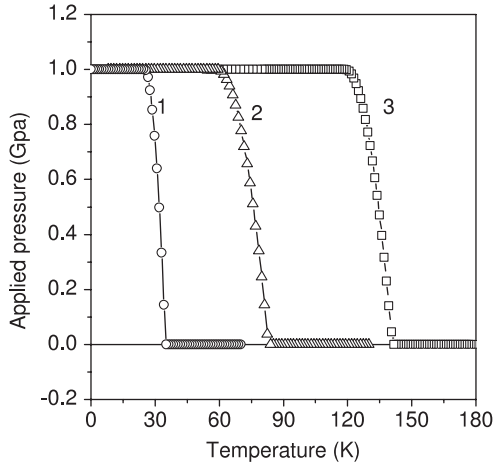

Figure 3. Pressure variation for calculating $[\Delta S]_M$ and $[\Delta T_{ad}]_M$ in the compounds $ErCo_2$, (curve 1) $HoCo_2$ (curve 2) and $DyCo_2$ (curve 3) shown in figure 4.

the applied pressure gets smaller or the magnetic field gets larger.

Similar calculations of the magnetocaloric effect in $HoCo_2$ and $DyCo_2$ have been done for applied pressure variations according to the processes respectively shown by curves 2 and 3 in figure 3. Again, the chosen temperatures to change the pressure lie around the magnetic ordering temperatures, where the competition between magnetic field and pressure to establish the magnetic order is strong. In figures 4(a) and (b) are respectively depicted the magnetocaloric potentials $[\Delta S]_M$ and $[\Delta T_{ad}]_M$ in ErCo, $HoCo_2$ and $DyCo_2$, calculated for magnetic field variation from 0 to 5 T and pressure variation according to the processes shown in figure 3. From figure 4(a), a broadening of all $[\Delta S]_M$ curves around the magnetic ordering temperature can be observed. This behavior is important for magnetic refrigerators operating in the Ericsson cycle. It should be said that similar behavior in the $[\Delta S]_M$ curve has also been observed in composite materials [21, 22] made up of more than one type of magnetic materials with different magnetic ordering temperatures.

In figures 5(a) and (b) are plotted the barocaloric potentials $[\Delta S]_B$ and $[\Delta T_{ad}]_B$ in $ErCo_2$, calculated for a fixed magnetic field of 1 T and pressure variation from 1.0 to 0 GPa (solid lines). For the sake of comparison, the corresponding magnetocaloric potentials $[\Delta S]_M$ and $[\Delta T_{ad}]_M$ calculated at ambient pressure and for a magnetic field variation from 0 to 1 T (dashed lines) have also been plotted in these figures. It can be observed that the peaks of the barocaloric potentials are larger than the peaks of the magnetocaloric potentials. Experimental data of the barocaloric potentials $[\Delta S]_B$ and $[\Delta T_{ad}]_B$ in $ErCo_2$ are necessary to confirm or reject the present theoretical calculations. It should be mentioned that it is expected that the curves of the barocaloric potentials in $ErCo_2$, like the magnetocaloric ones, exhibit small values at low temperatures. Therefore, the values of the calculated barocaloric potentials $[\Delta S]_B$ and $[\Delta T_{ad}]_B$ shown in figures 5(a) and (b) can be somewhat exaggerated at low temperatures, due to the fact that the magnetoelastic coupling is considered here, as a fixed parameter of the model. Similar behavior is also observed in the barocaloric potentials, not shown in this paper, for the compounds $HoCo_2$ and $DyCo_2$.

In conclusion, the magnetocaloric effect under applied pressure as well as the barocaloric effect in the compounds $ErCo_2$, $HoCo_2$ and $DyCo_2$ has been discussed in this work. The theoretical calculations show that (i) an applied pressure of 1.0 GPa shifts the peaks of the magnetocaloric potentials $[\Delta S]_M$ and $[\Delta T_{ad}]_M$ to lower temperatures without substantial changes in their magnitudes; (ii) the barocaloric potentials $[\Delta S]_B$ and $[\Delta T_{ad}]_B$ around the magnetic ordering temperature are as large as their magnetocaloric counterparts; (iii) the magnetocaloric potentials $[\Delta S]_M$ and $[\Delta T_{ad}]_M$ under simultaneous variation of the applied magnetic field and pressure exhibit special features depending on the specific procedure of magnetic field and pressure variation. Whether or not this new principle proves its practical application in magnetic refrigeration, it is very interesting from the fundamental physics point of view to study the magnetocaloric

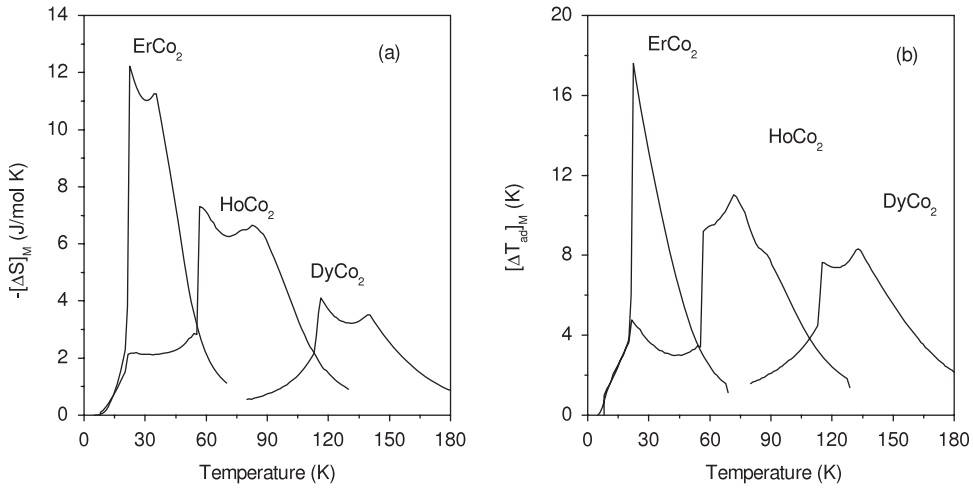

Figure 4. Magnetocaloric potentials $[\Delta S]_M$ (a) and $[\Delta T_{ad}]_M$ (b) in the compounds $ErCo_2$, $HoCo_2$ and $DyCo_2$ for magnetic field variation from 0 to 5 T and pressure variation from 0 to 1.0 GPa according to the processes shown in figure 3.

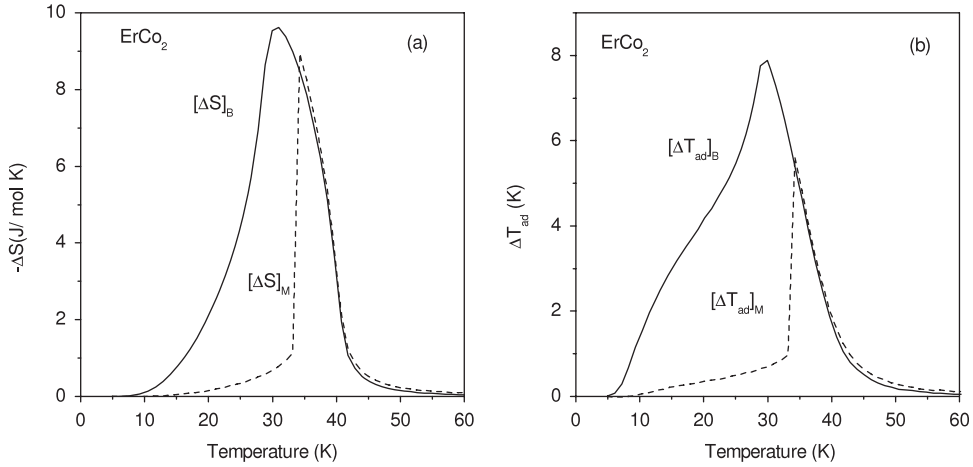

Figure 5. Barocaloric potentials $[\Delta S]_B$ (a) and $[\Delta T_{ad}]_B$ (b) in the compound $ErCo_2$ for a fixed magnetic field of 1 T and pressure variation from 1.0 to 0 GPa (solid lines). Dashed lines represent the magnetocaloric potentials $[\Delta S]_M$ and $[\Delta T_{ad}]_M$ calculated at ambient pressure and magnetic field variation from 0 to 1 T.

effect changing both external magnetic field and applied pressure.

Acknowledgments

This work has been performed under the auspices of the Brazilian agencies CNPq and FAPERJ.

References

[1] Tishin A M and Spichkin Y I 2003 *The Magnetocaloric Effect and its Applications* 1st edn (Bristol: Institute of Physics Publishing)
[2] Gschneidner K A Jr, Pecharsky V K and Tsokol A O 2005 *Rep. Prog. Phys.* **68** 1479
[3] Müller K A, Fauth F, Fischer S, Koch M, Furrer A and Lacorre P 1998 *Appl. Phys. Lett.* **73** 1056
[4] de Oliveira N A 2007 *Appl. Phys. Lett.* **90** 052501
[5] Wada H, Tomekawa S and Shiga M 1999 *J. Magn. Magn. Mater.* **196/197** 689
[6] Wada H, Tanabe Y, Shiga M, Sugawara H and Sato H 2001 *J. Alloys Compounds* **316** 245
[7] Herrero-Albillos J, Bartolomé F, Garcia L M, Casanova F, Labarta A and Batlle X 2006 *Phys. Rev.* B **73** 134410
[8] Giguerre A, Foldeaki M, Schnelle W and Gmelin E 1999 *J. Phys.: Condens. Matter* **11** 6969
[9] Duc N H and Kim Anh D T 2002 *J. Magn. Magn. Mater.* **242–245** 873
[10] Singh N K, Kumar P, Suresh K G, Nigam A K, Coelho A A and Gama S 2007 *J. Phys.: Condens. Matter* **19** 036213
[11] de Oliveira N A, von Ranke P J, Tovar Costa M V and Troper A 2002 *Phys. Rev.* B **66** 094402
[12] de Oliveira N A, von Ranke P J and Troper A 2004 *Phys. Rev.* B **69** 064421
[13] Kittel C 1960 *Phys. Rev.* **120** 335
[14] Duc N H, Givord D, Lacroix C and Pinettes C 1992 *Eur. Phys. Lett.* **20** 47
[15] Tishin A M and Spichkin Y I 2003 *The Magnetocaloric Effect and its Applications* 1st edn (Bristol: Institute of Physics Publishing) pp 232–4
[16] Lea K R, Leask M J M and Wolf W P 1962 *J. Phys. Chem. Sol.* **23** 1381
[17] Stevens W H 1952 *Proc. Phys. Soc. London* A **65** 209
[18] de Oliveira N A 2004 *Eur. Phys. J.* B **40** 259
[19] Syschenko O, Fujita T, Sechovsky V, Divis M and Fujii H 2001 *J. Magn. Magn. Mater.* **226–230** 1062
[20] Gignoux D, Givord F and Lemaire R 1975 *Phys. Rev.* B **12** 3878
[21] Hashimoto T, Kuzuhara T, Sahashi M, Inomata K, Tomokiyo A and Yayama H 1987 *J. Appl. Phys.* **62** 3873
[22] Smaili A and Chahine R 1996 *Adv. Cryog. Eng.* **42** 445